

Size of Micelles Determined by Static Fluorescence Quenching

Jiann-Jong Jeng (鄭建中), Jin-Ming Chen* (陳錦明) and Chung-Yuan Mou* (牟中原)
Department of Chemistry, National Taiwan University, Taipei, Taiwan 10764, Republic of China

We developed a new method to measure the average aggregation number of large rod-like micelles using static fluorescence self-quenching of a solubilized fluorophore. The method is based on the increase of self-quenching of micelle-solubilized pyrene through excimer formation. We consider the effect of random distribution of pyrene in micelles and the micellar size distribution. The measured average aggregation $\langle n \rangle_M$ is based on a new M-weighted averaging similar to our exponential-weighted averaging in the transient decay method. We apply this method to study the effect of a large concentration of salt on the average aggregation behavior of sodium dodecyl sulfate (SDS) and cetyl tetraammonium bromide (CTAB). The sizes increase with increasing ionic concentrations. For SDS, we used the thermodynamic model developed by Missel et al. to calculate $\langle n \rangle_M$ which we compare with experimental results.

INTRODUCTION

Micelles are small aggregates of amphiphilic molecules in solution. The fundamental problem of the structure of micelle¹ is to understand its size and shape distributions in terms of molecular interactions, that is, the hydrophobic/hydrophilic balance. It has become possible to a gain detailed understanding of the structure of a micelle on the molecular level following extensive theoretical and experimental attacks. Experimentally, one can now measure micellar size, shape and inter-micellar interactions by neutron (light) scattering^{2,3} and fluorescence probe techniques^{4,5} in addition to various traditional techniques.⁶

According to the fluorescence method, the determination of the micellar size is based on the quenching of fluorescence of a micelle-solubilized fluorophore, by the appropriate micelle-solubilized quencher. Pyrene self-quenching via excimer formation is commonly used for this purpose. The method is based on increased excimer formation in the micelle upon light excitation. This phenomenon can be measured from the increased fluorescence yield of the excimer or the increased fluorescence decay rate of excited monomer. The fluorophore generally used is pyrene because of its large singlet lifetime and efficient excimer formation in the liquid phase. With this technique, one can measure the large increase of aggregation number of an ionic micelles in concentrated ionic solution.⁵ The excimer yield is found to increase with increasing salt concentration. As the total amount of pyrene and surfac-

tants are kept constant, this increase can arise only from the increase probability of binary encounters between pyrene molecules in the micellar phase. As inter-micelle exchange is slow (microseconds) compared to fluorescence decay, one thus concludes that there is an appreciable increase of micellar size upon increasing salt concentration such that average number of pyrene molecules within each micelle becomes larger. The fluorescence quenching method has several advantages over other methods. Whereas light scattering, centrifugation and other methods are generally affected by intermicellar interactions, which may be appreciable in the case of ionic micelles, fluorescence methods are practically independent of interactions between micellar aggregates.

There are two methods of measuring fluorescence quenching, static and dynamic. The latter method gives us time-resolved variation of spectra, so it involves more dynamical information. It also requires complicated instrumentation and computations for evaluation of the data. In this paper, we are concerned with the application of the static fluorescence quenching method to micellar solutions. This method was first developed by Turro and Yekta,⁷ Infelta et al.⁸ and later by Malliaris;⁹ it is based on a relationship of the Stern-Volmer type modified by a Poisson distribution of the fluorophores in micelles. The instrumentation is simple and readily available. The determination of micellar size in previous applications were mainly restricted to monodispersed micelles.¹⁰ The purpose of our work has been to extend the static fluorescence

Dedicated to Professor Sheng-Lieh Liu (劉盛烈) on the occasion of his eightieth birthday.

* Present Address: Synchrotron Radiation Research Center (SRRC), Hsinchu, Taiwan.

method to poly-dispersed rod-like micelles. We demonstrate the potential and range of application of this technique in the determination of micellar size distribution for ionic micelles of sodium dodecyl sulfate (SDS) and cetyl tetra-ammonium bromide (CTAB).

For ionic micelles (cationic and anionic) in aqueous solution, the optimum size is determined by two factors.¹¹ One is the electrostatic effect of a simple salt due to the binding of counterions on the micellar surface, and the other is the hydrophobic interaction of the hydrocarbon chain which is related to the change of hydrogen bonding in water. When one increases the concentration of a simple salt added to a micellar solution, the effect is to decrease electrostatic repulsion between ionic head groups. The result is to favor micelle growth into a rod-like shape. A distinct feature of micelles which grow into long rods is pronounced polydispersity in size distribution. The fluorescence decay in this polydispersed micelles is different from those of monodispersed micelles, as discussed by Almgren et al.¹²

We⁵ have previously used pyrene as a fluorescence probe to study the effect of simple electrolytes on the average aggregation number of simple anionic micelles, sodium dodecylsulfate (SDS), sodium tetradecylsulfate (STDS) and lithium dodecylsulfate (LiDS) over the range of ionic concentration 0 to 0.8 M. We measured transient fluorescence decay upon excitation by a pulsed laser. We obtained by this technique an exponential weighted average aggregation number $\langle n \rangle_e$; it was smaller than the mass-weighted average aggregation number for rod-like poly-dispersed micelles. We apply here the static fluorescence technique and find a new average micellar aggregation number $\langle n \rangle_M$. We examine the systems of SDS and CTAB upon addition of large concentrations of strong electrolytes.

We have observed the increase of ionic size with increasing ionic concentration, in agreement with light scattering results. We compare our results with prediction of a thermodynamic model.

STATIC FLUORESCENCE QUENCHING IN POLYDISPERSE MICELLES

In many papers^{5,7,8} the monomer fluorescence decay has been related to the average number of fluorophores in each micelle. We follow here the analysis of Atik et al.¹³ The kinetic scheme consists of the following processes:

reaction	kinetic const
$M_n F_m \rightarrow M_n F^* F_{m-1}$	excitation of the fluorophore $\gamma_{m_n} I_a$
$M_n F^* F_{m-1} \rightarrow M_n F_m + h$	monomer fluorescence k_1
$M_n F^* F_{m-1} \rightarrow M_n F_2^* F_{m-2}$	excimer formation $(m_n - 1) k_E$
$M_n F_2^* F_{m-2} \rightarrow M_n F^* F_{m-1}$	excimer dissociation k_E
$M_n F_2^* F_{m-2} \rightarrow M_n F_m + h$	excimer fluorescence k_1'

Here $M_n F_m$ represents m fluorophores in a micelle of size n ; m_n denotes the occupation number of fluorophores in a micelle of size n ; γ_{m_n} is the fraction of m fluorophores in a micelle of size n ; k_1 , k_E , k_E and k_1' are the rate constants for monomer fluorophore decay, excimer formation, excimer dissociation and excimer decay, respectively. I_a is the incident light intensity. We assume that

- (1) pyrene dissolves only in micellar phase;
- (2) there is an independent random distribution of pyrene in the micelles; that is, they follow a Poisson distribution

$$f(m') = \frac{\langle m \rangle^{m'} e^{-\langle m \rangle}}{m'!} \quad (1)$$

in which $\langle m \rangle$ is the average number of pyrene in each micelle and m' is the number of pyrene molecule in a micelle;

- (3) solubilization of pyrene occurs to only a minor extent such that it does not change the size and structure of the micelles;
- (4) exchange of pyrene between micelles is slow so that it does not affect fluorescence quenching behavior.

We derive the relation for the decay of fluorescence⁵

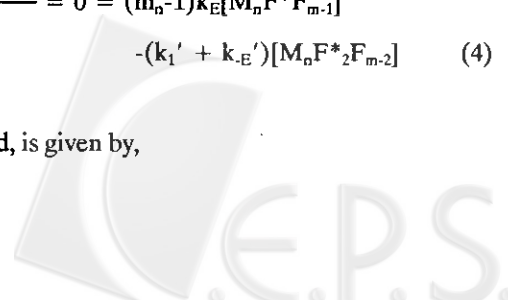
$$\ln \frac{I(t)}{I(0)} = \langle n \rangle_e \{ \exp(-k_E t) - 1 \} - k_1 t \quad (2)$$

Previously, we used the technique of temporal decay of monomer fluorescence and with Eq. 2 we measured the average aggregation number $\langle n \rangle_e$ of SDS and other surfactants. Here we consider the steady-state method. Under steady-state conditions the kinetic scheme gives us

$$\frac{d[M_n F^* F_{m-1}]}{dt} = 0 = \gamma_{m_n} I_a - [k_1 + (m_n - 1)k_E][M_n F^* F_{m-1}] + k_E[M_n F_2^* F_{m-2}] \quad (3)$$

$$\frac{d[M_n F_2^* F_{m-2}]}{dt} = 0 = (m_n - 1)k_E[M_n F^* F_{m-1}] - (k_1' + k_E)[M_n F_2^* F_{m-2}] \quad (4)$$

γ_{m_n} , as defined, is given by,



$$\gamma_{m_n} = \frac{m_n \alpha_{m_n}}{\sum_{n=1}^{\infty} \sum_{m_n=1}^{\infty} m_n \alpha_{m_n}} \quad (5)$$

and α_{m_n} is the population of m fluorophores in micelles of size n following the Poisson distribution,

$$\alpha_{m_n} = \frac{(\bar{m}_n)^{m_n} \exp(-\bar{m}_n)}{m_n!} \quad (6)$$

Then the quantum yield of monomer fluorescence for micellar size n is given by,

$$\Phi_{m_n}^M = k_f [M_n F^* F_{m-1}] / \gamma_{m_n} I_a \quad (7)$$

in which k_f is the radiative rate constant of the excited monomer fluorophore. From eqs (3), (4) and (7), we obtain,

$$\Phi_{m_n}^M = \frac{k_f}{k_i + (m_n - 1) k_E k_i' / (k_E + k_i')} \quad (8)$$

When there is only one fluorophore in each micelle, obviously we have

$$\Phi_M^o = k_f / k_i = k_f \tau_f, \text{ with } \tau_f = k_i^{-1}$$

Therefore,

$$\Phi_{m_n}^M = \Phi_M^o [1 + \beta k_E \tau_f (m_n - 1)]^{-1}, \text{ and } \beta = \frac{k_i'}{k_E + k_i'} \quad (9)$$

Then the total quantum yield of monomer fluorescence is given by

$$\begin{aligned} \Phi_M &= \sum_n P(n) \sum_{m_n} \gamma_{m_n} \Phi_{m_n}^M \\ &= \sum_n P(n) \sum_{m_n} \frac{m_n \alpha_{m_n}}{\bar{m}_n} \Phi_{m_n}^M \end{aligned} \quad (10)$$

in which $P(n)$ is the size distribution of the micelles. For the quantum yield of excimer fluorescence, a similar procedure yields

$$\Phi_{M_n}^E = \Phi_E^o / \{1 + [\beta k_E \tau_f (m_n - 1)]^{-1}\} \quad (11)$$

$$\Phi_E^o = k_f' \tau_f' \quad (12)$$

with $\tau_f' = (k_i')^{-1}$; k_f' is the radiative rate constant of excimer. The total quantum yield of excimer fluorescence is then given by

$$\Phi_E = \Phi_E^o \sum_n P(n) \sum_{m_n=2}^{\infty} \frac{(\bar{m}_n)^{m_n-1} \exp(-\bar{m}_n)}{(m_n-1)! \{1 + [\beta k_E \tau_f (m_n-1)]\}^{-1}} \quad (13)$$

The quantum yield of monomer fluorescence (Eq. 10) is written in the form,

$$\Phi_M = \Phi_M^o \sum_n P(n) \sum_{m_n=1}^{\infty} \frac{(\bar{m}_n)^{m_n-1} \exp(-\bar{m}_n)}{(m_n-1)! [1 + \beta k_E \tau_f (m_n-1)]} \quad (14)$$

The sum over m_n in eq(14) is made in closed form and the result is a confluent hypergeometric function. We omit the details;¹⁴ the result is

$$\frac{\Phi_M}{\Phi_M^o} = \sum_n P(n) e^{-\bar{m}_n} M(d, d+1, \bar{m}_n) \quad (15)$$

in which $M(d, d+1, \bar{m}_n)$ is the confluent hypergeometric function and the parameter d is given by $d = (\beta k_E \tau_f)^{-1}$. Similarly, the quantum yield for excimer fluorescence is given by

$$\frac{\Phi_E}{\Phi_M^o} = \sum_n P(n) e^{-\bar{m}_n} \bar{m}_n (d+1)^{-1} M(d+1, d+2, \bar{m}_n) \quad (16)$$

The apparent concentration of dissolved pyrene be C_{py} ; cmc is the critical micelle concentration where the micelles begin formation and C is the surfactant concentration; then the average \bar{m}_n is given by

$$\frac{\bar{m}_n}{n} = \frac{C_{py}}{C - cmc} \quad (17)$$

Thus eq. (15) is written as

$$\frac{\Phi_M}{\Phi_M^o} = \sum_n P(n) \exp(-nC_{py}/(C - cmc)) M(d, d+1, nC_{py}/(C - cmc))$$

This equation gives us the monomer fluorescence yield in terms of a weighted average over the micellar size distribution. The weighting function is different from that in Eq. 2. Thus we define a weighted average aggregation number $\langle n \rangle_M$ from the experimentally measured fluorescence intensity quenching,

$$I/I_o = \exp(-\langle n \rangle_M C_{py}/(C - cmc)) M(d, d+1, \langle n \rangle_M C_{py}/(C - cmc)) \quad (18)$$



Eq. (18) is to be solved iteratively to calculate the M-weighted size $\langle n \rangle_M$.

EXPERIMENTAL SECTION

Pyrene (Riedel-DeHaen) was separated on column of silica gel and collected after vacuum sublimation as reported previously⁵. Both surfactants, SDS and CTAB, were from Merck; the purity of SDS is exceeded than 99%; it was used without purification. We recrystallized twice CTAB; the HPLC determination showed that our CTAB sample purity is exceeded than 99.5%. All salts (NaCl and NaBr) were recrystallized twice.

Preparation of sample: Pyrene was dissolved in hexane, then hexane was pumped out to leave a thin layer of pyrene on the flask surface. A detergent solution was then added to this flask and stirred at 50°C for three days to ensure complete dissolution. The samples were extensively de-oxygenated by nitrogen bubbling before measurement of the fluorescence spectrum. The fluorescence spectra were recorded on a fluorometer (Perkin-Elmer LS-5) with data station (Perkin-Elmer 3600). All samples were thermostated within 0.1°C. Care was taken to avoid the inner filtering effect.

All experiments were done with constant concentrations of pyrene and surfactant whereas the salt concentration was varied. The emission between 370 nm and 420 nm is that of monomer pyrene, the emission band centered at 475 nm was due to excimer.

To obtain the proper value of I/I_0 , we made many measurements of fluorescence at small concentrations of pyrene such that the intensity varied linearly with pyrene concentration. We thus determined the intensity for the hypothetical state that there was no excimer formation.

RESULTS

In order to use Eqs. 15 and 18 to calculate $\langle n \rangle_M$, one needs the values of rate constants, k_1 , k_E , etc., and cmc. As we have measured them previously,⁵ we used these values. Some values are interpolations of literature data. The values of CMC and rate constants are listed in Tables 1 and 2.

In Table 3, we list the results of the measured values of monomer quenching ratio I/I_0 for various combinations of surfactant and salt at many different temperatures. The aggregation numbers $\langle n \rangle_M$ calculated from Eq. 18 for SDS and CTAB at various temperatures, salt concentrations and

Table 1. CMC and Kinetic Parameters of SDS Micellar System for Various Salt Concentration at Different Temperatures

T/°C	CMC/10 ⁻³ M	K _E /10 ⁷ s ⁻¹ *	K _J /10 ⁶ s ⁻¹ *	K _I /10 ⁶ s ⁻¹
(a) [NaCl] = 0.0 M				
30	8.25*	2.0	2.29	3.16
35	8.43	2.3	2.43	3.08
40	8.60*	2.7	2.56	3.12
50	9.03	4.0	3.31	3.94
60	10.00	4.0	4.45	3.86
70	12.00	4.5	4.32	4.58
(b) [NaCl] = 0.2 M				
30	0.88*	2.0	2.45	3.56
35	0.91	2.3	2.60	3.52
40	0.93	2.7	2.72	3.51
50	0.97	3.3	3.36	4.00
60	1.10	3.6	3.58	3.96
70	1.26	3.9	4.19	4.23
(c) [NaCl] = 0.4 M				
30	0.57*	2.0	2.61	3.63
35	0.58	2.4	2.80	3.78
40	0.60	2.6	2.89	3.55
50	0.63	3.0	3.41	3.76
60	0.70	3.2	3.71	3.86
70	0.81	3.4	4.07	4.48
(d) [NaCl] = 0.5 M				
30	0.53*	2.0	2.69	3.87
35	0.54	2.4	2.89	3.73
40	0.55*	2.6	2.97	3.77
50	0.58	2.9	3.44	3.99
60	0.65	3.0	3.78	4.46
70	0.75	3.1	4.01	4.73
(e) [NaCl] = 0.8 M				
30	0.36*	1.0	2.29	3.53
35	0.37	1.2	2.51	3.46
40	0.37*	1.3	2.56	3.38
50	0.39	1.6	2.70	3.51
60	0.44	2.0	2.67	3.50
70	0.51	2.3	2.78	3.73

*The values are interpolations of literature data.

surfactant concentrations are listed in Table 4. The aggregation number increases with increasing salt concentra-

Table 2. CMC and Kinetic Parameters of CTAB Micellar System at Different Temperatures

T/°C	CMC(10 ⁻³)/M	K _E (10 ⁶)/S ⁻¹	K _I (10 ⁶)/S ⁻¹
22	0.8*	0.47*	5.8*
30	0.8	0.61	6.48
35	0.8	0.76	6.71
40	0.8	0.95	6.93
50	0.8	1.34	7.41
60	0.8	1.73	8.00
70	0.8	2.11	8.70

*The values are interpolations of literature data.

Table 3. Measured Values of Monomer Quenching Ratio I/I_0 for Various Combinations of Surfactant and Salt at Different Temperatures

(a) I/I_0 values of SDS micelles system, [SDS] = 0.0625 M, [NaCl] variable						
$T/^\circ\text{C}$	I/I_0	0.0	0.2	0.4	0.5	0.8
30		0.813±0.012	0.729±0.015	0.786±0.012	0.687±0.01	0.587±0.015
35		0.793±0.012	0.729±0.015	0.720±0.01	0.698±0.02	0.637±0.032
40		0.798±0.01	0.738±0.01	0.727±0.017	0.722±0.01	0.639±0.032
50		0.829±0.02	0.756±0.02	0.773±0.015	0.760±0.03	0.675±0.034
60		0.803±0.023	0.740±0.02	0.762±0.015	0.742±0.045	0.716±0.06
70		0.780±0.04	0.744±0.015	0.781±0.02	0.730±0.09	0.739±0.09

(b) I/I_0 values of CTAB micelles system, [CTAB] = 0.0625 M, [NaBr] Variable						
$T/^\circ\text{C}$	I/I_0	0.0	0.2	0.4	0.5	0.8
22		0.810±0.017	0.715±0.02	0.634±0.013		
30		0.795±0.012	0.703±0.017	0.624±0.012	0.649±0.04	0.596±0.015
35		0.799±0.014	0.697±0.014	0.615±0.013	0.635±0.042	0.590±0.01
40		0.790±0.016	0.701±0.014	0.658±0.02	0.621±0.03	0.583±0.012
50		0.801±0.01	0.696±0.015	0.643±0.02	0.606±0.036	0.557±0.011
60		0.787±0.02	0.700±0.012	0.627±0.02	0.613±0.038	0.537±0.012
70		0.797±0.026	0.712±0.01	0.633±0.022	0.637±0.029	0.542±0.016

(c) I/I_0 values of CTAB micelles system, [NaBr] = 0.0 M, [Pyrene] ~ 10^{-4} M				
$T/^\circ\text{C}$	I/I_0	[CTAB] = 0.0375 M	[CTAB] = 0.0625 M	[CTAB] = 0.10 M
22		0.785±0.014	0.810±0.017	0.769±0.01
30		0.778±0.02	0.795±0.012	0.768±0.01
35		0.766±0.02	0.799±0.014	0.750±0.01
40		0.768±0.015	0.790±0.016	0.752±0.01
50		0.745±0.014	0.801±0.01	0.742±0.01
60		0.758±0.01	0.787±0.02	0.740±0.01
70		0.728±0.022	0.797±0.026	0.733±0.01

(d) I/I_0 values of SDS micelles system, [NaCl] = 0.5 M, [Pyrene] ~ 10^{-4} M			
$T/^\circ\text{C}$	I/I_0	[SDS] = 0.0347 M	[CTAB] = 0.0625 M
30		0.430±0.021	0.813±0.012
35		0.422±0.02	0.793±0.012
40		0.431±0.02	0.798±0.01
50		0.470±0.015	0.829±0.02
60		0.480±0.02	0.803±0.023
70		0.480±0.015	0.780±0.04

tion for both systems. At the salt concentration 0.4 M, there seems to be an abrupt change of micellar size. The micellar size decreases as the temperature is increased as shown in Figs. 1 and 2. The aggregation number of CTAB increases with concentration of CTAB at all temperatures shown in Fig. 3. To check the sensitivity of this method to oxygen quenching, we performed some experiments without degassing. The calculated aggregation number is compared with the degassing results, these are listed in Table 5. As there appears no significant difference, it may

be safe to measure aggregation number without the cumbersome degassing operation.

DISCUSSION

We review the problem of large aggregation of micelles at high ionic strength. For the case of SDS in high concentration of NaCl, various techniques give similar results at small ionic concentration (0 to 0.2 M), but for salt con-

Table 4. Measured Aggregation Number $\langle n \rangle_M$ for Various Systems(a) $\langle n \rangle_M$ of SDS micelles system, [SDS] = 0.0625 M, [NaCl] variable

[NaCl]/M	0.0	0.2	0.4	0.5	0.8
T/°C					
31	87±6	160±10	190±9	200±8	304±25
35	90±6	150±10	166±7	183±10	250±28
40	90±6	142±6	152±11	163±7	210±22
50	74±10	134±12	128±9	138±19	198±25
60	79±11	133±13	121±9	138±27	165±35
70	88±19	134±9	115±12	152±40	144±45

(b) $\langle n \rangle_M$ of CTAB micelles system, [CTAB] = 0.0625 M, [NaBr] variable

[NaBr]/M	0.0	0.2	0.4	0.5	0.8
T/°C					
22	148±15	209±10	270±13		
31	144±10	202±10	262±13	328±40	365±14
35	136±10	199±12	252±11	319±35	345±12
40	130±12	189±11	212±15	306±33	322±13
50	123±6	177±11	206±14	281±34	311±12
60	118±13	169±8	200±14	256±34	305±12
70	110±16	157±6	195±15	230±23	292±15

(c) $\langle n \rangle_M$ of SDS micelles system, [NaCl] = 0.5 M

[SDS]/M	0.0347	0.0625
T/°C		
31	198±8	201±12
35	150±10	196±11
40	163±7	182±10
50	138±19	167±7
60	138±27	158±9
70	152±40	158±9

(d) $\langle n \rangle_M$ of CTAB micelles system, [NaBr] = 0.0 M

[CTAB]/M	0.0375	0.0625	0.10
T/°C			
22	82±8	148±15	241±12
31	80±9	144±10	232±11
35	80±9	136±10	235±11
40	75±7	130±12	224±10
50	75±4	123±6	217±10
60	70±4	118±13	210±9
70	76±4	110±16	213±9

Table 5. Comparison of Measured Aggregation Number $\langle n \rangle_M$ under Degassing and Non-degassing Treatments

(a) [SDS] = 0.0625 M, [NaCl] = 0.0 M

T/°C	31	35	40	50	60	70
DEGAS	92	90	90	85	82	95
NONDEGAS	85	90	89	75	77	85

(b) [SDS] = 0.0625 M, [NaCl] = 0.4 M

T/°C	31	35	40	50	60	70
DEGAS	200	172	148	118	119	115
NONDEGAS	195	170	160	128	125	120

centration above 0.3 M there are results of two types. Mysels and Princen,¹⁵ using a conventional light scattering technique, obtained a mean aggregation number about 60 without NaCl which increases gradually to 140 at [NaCl] = 0.5 M near the critical micelle concentration. Ikeda et al.¹⁶ found a large increase of aggregation number up to 1000 at 35°C and [NaCl] = 0.8 M. The interpretation gradually shifts to rodlike micelle at a large concentration of salt. Mazer et al.¹⁷ used quasi-elastic light scattering to study the effect of NaCl on SDS micelles. They found that for SDS concentration at 0.069 M, T = 25°C, an increase of ionic concentration in the range 0 - 0.6 M resulted in an increase

of the aggregation number from 80 to 1000. These later results disagree with the results by fluorescence quenching which agree more those from with viscosity and earlier light scattering measurements, Based on the later results, many workers have interpreted the growth of micelle size as an

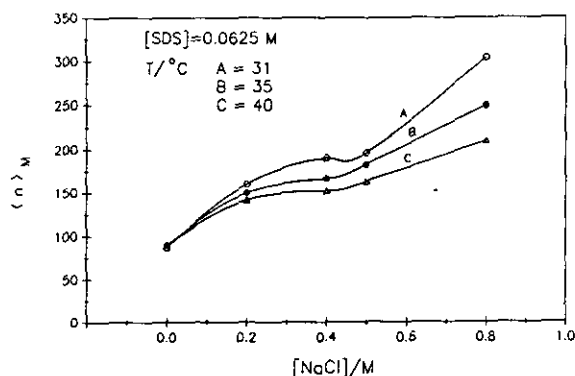


Fig. 1. Average aggregation number $\langle n \rangle_M$ for SDS at various NaCl concentrations and temperatures.

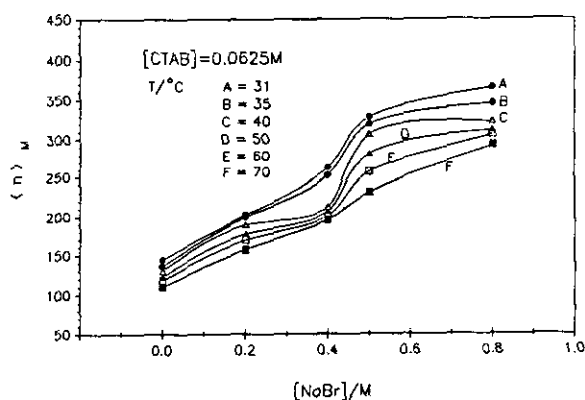


Fig. 2. Average aggregation number $\langle n \rangle_M$ for CTAB at various NaBr concentrations and temperatures.

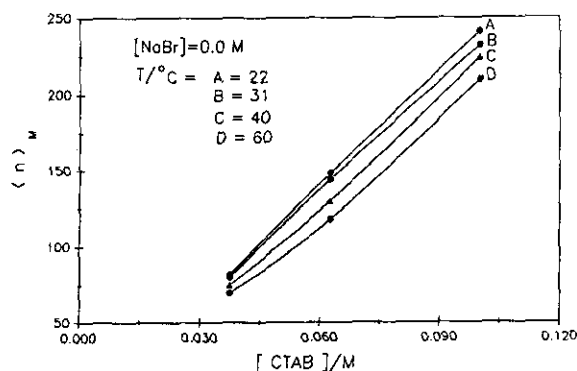


Fig. 3. Average aggregation number $\langle n \rangle_M$ for CTAB at various concentrations and temperatures, when [NaBr] = 0.0 M.

elongation of large rodlike micelles with a single connecting interior at high ionic strength. This concept began in the theoretical consideration of Stigter.¹⁸ Later Missel et al.¹⁹ proposed a simple ladder model for such spherocylindrical micelles; they used only two independent parameters to characterize the chemical potential of the micelle and to fit well the average size of SDS obtained from diffraction data. The model is based on multiple equilibrium between monomer surfactant (S) and micelle of size n . We have previously^{5a} used this model to explain our data of $\langle n \rangle_e$; we apply this model to the present results.

X_1 and X_n are the molar fractions of monomer surfactant and micelle of size n ; we have

$$X_n = X_1^n \exp(-(\mu_n^\circ - n\mu_1^\circ)/RT) \quad (19)$$

in which μ_n° and μ_1° are, respectively, the standard parts of the chemical potential. For a spherocylindrical micelle with n_0 monomers in the end caps and $n-n_0$ in the cylindrical part, the chemical potential change is separated into the cap part and the cylindrical part

$$\begin{aligned} \mu_n^\circ - n\mu_1^\circ &= (\mu_{n_0}^\circ - n_0\mu_1^\circ) + (n-n_0)(\mu_n^\circ - \mu_1^\circ) \\ &= \Delta + (n-n_0)\delta \end{aligned} \quad (20)$$

and δ represents the equal-space change of Gibbs energy upon transfer of each monomer from solution to the cylindrical part of the micelle. Therefore the micellar distribution $P(n)$ is given by

$$P(n) = X_n / (\sum_n X_n) \quad (21)$$

Only two Gibbs energy parameters are needed to fit the size distribution. For SDS we use the parameters from Ref. 5.

In Fig. 4, we plotted the results of the model calculation with the experimental values for SDS at [NaCl] = 0.8 and 0.5 M. We did not attempt the model calculation for salt concentration less than 0.5 M as the micelles become less rodlike. One sees that the theoretical model agrees well with experimental results for the case of [NaCl] = 0.5 M. But for the larger micelles at [NaCl] = 0.8 M, they diverge at low temperatures. Why the model fails at low temperature is unknown but there is a similar tendency for the case of $\langle n \rangle_e$ in our previous work. We draw the attention of theorists to this problem so as to modify the ladder model to fit better our data. For comparison, we also plotted our previous results of $\langle n \rangle_e$ in the same figure. Although they are of different weighting, the two results

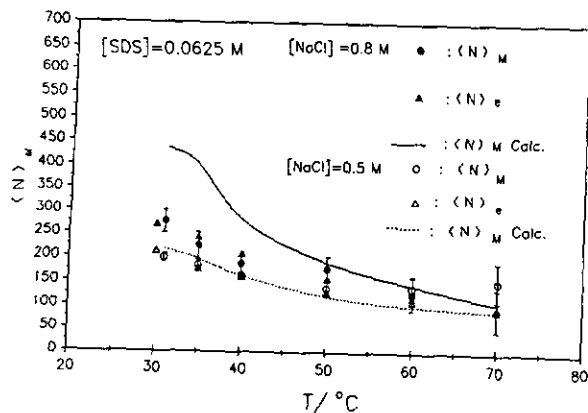


Fig. 4. Average aggregation numbers $\langle n \rangle_M$ and $\langle n \rangle_e$ for SDS at $[\text{NaCl}] = 0.5$ and 0.8 M, solid lines are the results of model calculation.

$\langle n \rangle_e$ and $\langle n \rangle_M$ are similar. But we do observe a small difference; at low temperature $\langle n \rangle_e$ tends to exceed $\langle n \rangle_M$ whereas at high temperature side the opposite is true.

ACKNOWLEDGMENT

This research was supported by a grant from the National Science Council of the Republic of China. We thank Professor Tong-In Ho for his loan of a fluorescence spectrometer.

Received July 12, 1991.

Key Words

Micellar solution; Critical micelle concentration; Fluorescence probe; Excimer formation; Exponent-weighted average aggregation number; Mass-weighted average aggregation number.

REFERENCES

1. For a reviews see (a) Wennerstrom, H.; Lindman, B. *Phys. Reports* **1979**, *52*, 1. (b) Evans, D. F.; Ninham, B. W. *J. Phys. Chem.* **1986**, *90*, 226. (c) Chevalier, Y.; Zemb, T. *Rep. Prog. Phys.* **1990**, *53*, 279. (d) Tanford, C. *The hydrophobic effect*; Wiley: New York **1980**.
2. Chen, S. H.; Lin, T.-L. In *Methods of Experimental Physics-Neutron Scattering in Condensed Matter Research*; Skold, K.; Price, D. L. Eds.; Academic: New York, **1987**; Vol 23B, Chapter 16.
3. Corti, M.; Degiorgio, V. *J. Phys. Chem.* **1981**, *85*, 1442.
4. Zana, R. *Surfactant Solutions, New Methods of Investigation*; Dekker: New York, **1987**.
5. (a) Chen, J. M.; Su, T. M.; Mou, C. Y. *J. Phys. Chem.* **1986**, *90*, 2418. (b) *idem.* *J. Chin. Chem. Soc.* **1989**, *36*, 319.
6. Ikeda, S.; Hayashi, S.; Imae, T. *J. Phys. Chem.* **1981**, *85*, 106.
7. See for example, (a) Eriksson, J. C.; Ljunggren, S.; Henrikson, U. *J. Chem. Soc., Faraday Trans 2* **1985**, *81*, 833. (b) Mitchell, D. J.; Ninham, B. W. *J. Chem. Soc., Faraday Trans 2* **1981**, *77*, 601.
8. Infelta, P. P.; Gratzel, M.; Thomas, J. K. *J. Phys. Chem.* **1974**, *78*, 190.
9. Malliaris, A. *Adv. Colloid Interfac. Sci.* **1987**, *27*, 153.
10. Infelta, P. P. *Chem. Phys. Lett.* **1979**, *61*, 88.
11. Rusanov, A. I. *Russian Chem. Rev.* **1989**, *58*, 169.
12. (a) Almgen, M.; Alsins, J.; Muktar, E.; Stam, J. V. *J. Phys. Chem.* **1988**, *92*, 4479. (b) Alsins, J.; Almgen, M. *J. Phys. Chem.* **1990**, *94*, 3062.
13. Atik, S. S.; Singer, L. A. *Chem. Phys. Lett.* **1978**, *59*, 519.
14. Jeng, J. J. Master's Thesis, National Taiwan University, June 1988.
15. Mysel, K. J.; Princen, L. H. *J. Phys. Chem.* **1959**, *63*, 1699.
16. Ikeda, S.; Hayashi, S.; Imae, T. *J. Phys. Chem.* **1981**, *85*, 106.
17. Mazer, N. A.; Benedek, G. B.; Carey, M. C. *J. Phys. Chem.* **1976**, *80*, 1075.
18. Stigter, D. *J. Phys. Chem.* **1966**, *70*, 1323.
19. Missel, P. J.; Mazer, N. A.; Benedek, G. B.; Young, C. Y.; Carey, M. C. *J. Phys. Chem.* **1980**, *84*, 1044.

